Int. J. Electrochem. Sci., 10 **(2015)** 5350 - 5357

International Journal of ELECTROCHEMICAL SCIENCE
www.electrochemsci.org

Short Communication

Preparation of $Rh_5@Pt_x/C$ Core-Shell Nanoparticles for Electrocatalytic Oxidation of Ethanol

Li Fang[1,*], *Jinlu He*[1], *Surin Saipanya*[2,*], *Xiaoping Huang*[1]

[1]School of Chemistry and Chemical Engineering, Shanxi University, Taiyuan, Shanxi, 030006, China.
[2]Department of Chemistry, Faculty of Science, Chiang Mai University, 50200, Thailand.
[*]E-mail: fangli@sxu.edu.cn; surin saipanya@hotmail.co.uk

Received: 22 January 2015 / *Accepted:* 15 April 2015 / *Published:* 27 May 2015

$Rh_5@Pt_x/C$ core-shell nanoparticles were prepared by a two-step hydrogen reduction process and characterized by cyclic voltammetry (CV) combined with X-ray diffraction (XRD) and transmission electron microscopy (TEM). The effects of the thickness of Pt shell on the catalytic performance for ethanol oxidation were investigated for activity performance evaluation. It was also found that Rh core was practically covered by Pt shell with a strong interaction between Rh and Pt although there was no PtRh alloy formation at the surface of the Pt shell during the deposition process for the catalyst preparation. The Rh core remarkably enhanced the catalytic activity of Pt shell and promoted the breaking of C-C bonds of ethanol resulting in relatively lower potential for the ethanol reaction. It can also be concluded that the current density of the oxidation peak on $Rh_5@Pt_5/C$ was ca. 64 % higher than that on Pt_5/C although they both showed rather similar characteristic peaks.

Keywords: Rh@Pt/C; Core-shell Structure; Direct Ethanol Fuel Cell; Electrocatalytic oxidation; Cyclic voltammetry

1. INTRODUCTION

Platinum-based binary and ternary alloys nanoparticles (such as PtRu, PtRh, PtRuRh, PtRuSn, PtRhSn, etc.) have been used as the anode catalysts in low-temperature ethanol fuel cell as they performed such a high catalytic activity and strong CO-poison tolerance [1-10]. Among them, Rh in PtRh bimetallic catalyst has been remarkably considered to be the most effective anode catalyst promoter for ethanol electrooxidation since there was found that Rh plays a key role in the reaction as following reasons. Firstly, the existence of Rh could accelerate the oxidation rate of CO_{ads} on Pt surface due to the bifunctional mechanism [10-12]; secondly, the special electronic effect between Rh atoms and their adjacent Pt atoms, which are able to improve the activity of the catalyst; thirdly, Rh

has particular contribution to the break of C-C bond of ethanol at low potential [13-18] and lastly, Rh could reduce the electrooxidation products formed at higher potential [16].

However, the PtRh alloy catalyst prepared with the traditional co-deposition method has some drawbacks as high content of precious metals would bring it to high cost of production and the activity still needs to be improved [17-18]. The catalyst preparation to maximize utilization of the catalytic ability of Pt and other metals needs to be taken into account. It was found that the Pt base core-shell structure nanoparticles (M@Pt ; M = Pd, Rh, Ru, etc.) could not only employ the electric catalytic ability of metals but also reduce the content of Pt amount [19-23]. There are some work have been done on core-shell nanoparticles of Pt-based catalysts possessing of higher surface area which in better catalytic performance were started as follows [16-20]. Oliveira *et al.* reported that the oxidation behaviors of small organic molecules on the Pt/Rh/Pt multilayers surface showed the catalytic activity increase for 295 % while the CV curve was the same as the pure Pt electrode [11]. Lima *et al*. prepared core-shell Pt/Rh/C prepared by electrodeposition method showed the oxidation of ethanol on the catalyst was at 150 mV negatively shift in comparison with that on RhPt/C alloy catalyst [15].

In this paper, the preparation of core-shell $Rh_5@Pt_x/C$ catalysts with different Pt contents was achieved by a two-step force deposition method and the results of CV combined with XRD and TEM were acquired for characterization. It was also shown that the thickness of Pt shell remarkably influences the catalytic activity on the ethanol electrooxidation reaction.

2. EXPERIMENTAL

2.1 Chemicals and reagents

Graphite powder was purchased from Alfa Aesar, chloroplatinic acid hexahydrate ($H_2PtCl_6 \cdot 6H_2O$ 99.9%) and rhodium chloride trihydrate ($RhCl_3 \cdot 3H_2O$) were purchased from Sigma-Aldrich, and all other reagents were of analytical grade and used without further purification. Milli-Qwater (18.2 MΩcm) was used for all solution preparation.

2.2 Catalyst preparation

Graphite powder was activated before use. Briefly, a certain amount of graphite was completely immersed in HCl solution for 24 h. The slurry was then washed with distilled water and vacuum filtered until no Cl^- ion presences and dried at 373 K in the oven. The obtained product was calcined in the air at 700 K for 4 h and then reduced at 423 K in H_2 gas.

To prepare $Rh_5@Pt_x/C$ nanoparticles, the activated graphite was firstly added into the H_2 bubbler filled with glycol aqueous solution (volume ratio of glycol and water was 2:1) and ultrasonic treated for 15 min. A certain volume of $RhCl_3$ solution (5×10^{-6} mol/L) was then added into the H_2 bubbler and reduced by ultra-pure H_2 flow for 1 h. After the Rh_5/C particles were obtained, the H_2PtCl_6 solution (7.7×10^{-3} mol/L) was added into the slurry with H_2 flow through for another 1 h and then washed with ultrapure water. The obtained catalysts was filtered and dried at 373 K and labeled as $Rh_5@Pt_x/C$ (x represents the mass ratio of Pt to the graphite amount)[10, 24].

2.3 Physical characterization

The $Rh_5@Pt_x/C$ core-shell catalysts were characterized by X-ray diffraction (XRD) using a Bruker D8 Advance operated with a Cu Kα source (λ = 0.154 nm) at 40 kV and 40 mA. The measurement was carried out in 2θ of 20°-70° at sweep rate of 5°/min. TEM images of the catalysts were recorded on a JEM-2100 (JEOL) microscope working at 200 keV.

2.4 Electrochemical measurement

The electrochemical experiments were performed in a conventional three-electrode system at room temperature using a CHI potentiostat (CHI 600C). A saturated calomel electrode (SCE) and Pt foil were used as reference and counter electrode, respectively. The working electrode was prepared by coating $Rh_5@Pt_x/C$ catalyst ink onto a glassy carbon electrode (GCE). The electrolyte solution (0.1 M H_2SO_4 or 0.1 M CH_3CH_2OH in 0.1 M H_2SO_4) was bubbled with N_2 (99.999 %) flow for at least 30 min to deoxygenate the solution before running cyclic voltammetry (CV) experiments. All CV profiles of the prepared catalysts were recorded at a sweep rate of 10 $mV \cdot s^{-1}$.

3. RESULTS AND DISCUSSION

3.1 XRD characterization

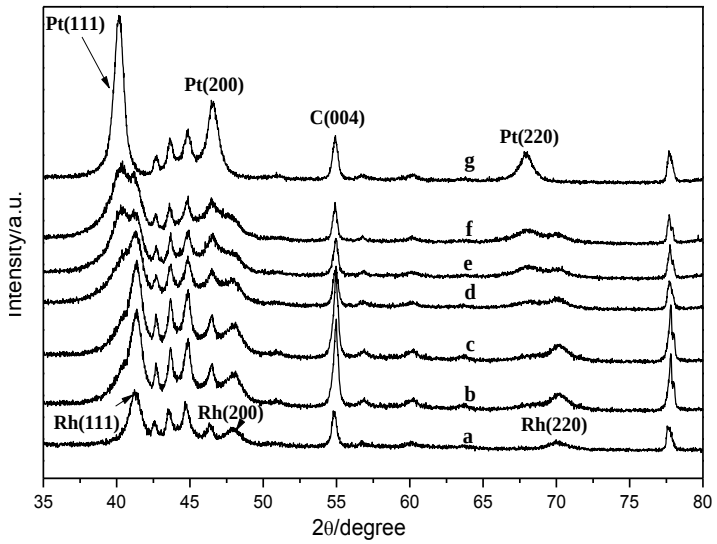

Figure 1. XRD patterns of the $Rh_5@Pt_x/C$ core-shell catalysts: (a) Rh_5/C, (b) $Rh_5@Pt_1/C$, (c) $Rh_5@Pt_2/C$, (d) $Rh_5@Pt_3/C$, (e) $Rh_5@Pt_4/C$, (f) $Rh_5@Pt_5/C$ and (g) Pt_5/C.

The XRD patterns of the $Rh_5@Pt_x/C$ catalysts with different Pt shell thicknesses are shown in Figure1. It is evidently seen that the peaks of Rh_5/C (Figure 1(a)) observed at 41.26°, 47.96° and 70.11° are assigned to Rh(111), Rh(200) and Rh(220), respectively. In Figure 1(g), the peaks of Pt_5/C

at 40.19°, 46.55° and 67.96° are assigned to Pt(111), Pt(200) and Pt(220), respectively. In Figure 1(b)-(f), an increase of Pt content (x = 1 to 5) in Pt shell shows an increase of diffraction peak intensities corresponding to Pt(111), Pt(200) and Pt(220) orderly whereas the intensity of Rh(111), Rh(200) and Rh(220) diffraction peaks gradually decrease and broaden. Interestingly, both of Pt(111) and Rh(111) diffraction peaks of $Rh_5@Pt_5/C$ (Figure1(f)) presented at 40.35° and 41.18° which deviate from the values of 2θ corresponding to pure Pt(111) and Rh(111), respectively, and they lean closer to one another. These indicate that the electronic effects of Pt and Rh changed because of the formation of Rh@Pt core-shell structure with the formation of PtRh alloy in the junction area between Rh layer and Pt layer. It is also worth mentioning that the intensity of Pt(111) is much stronger than that of Rh(111) although the content of both metals are comparable to each other. This could be ascribed to the weaker diffraction patterns of Rh core covered by the thick Pt shell thickness. It has been stated that the formation of Rh@Pt core-shell structure during the depositing process is normally followed the model of layer by layer. Although, the Pt growth on the surface of Rh_5/C might occur as a Volmer-Weber (3D crystallite growth) model [25] where the second layer starts before the first layer completes. Therefore, the Pt islands formation on the surface of Rh_5/C substrate can be occurred as the Pt would preferentially deposit on Pt islands rather than on those vacant Rh surfaces resulting in existing of some exposed parts of Rh_5/C surface [10, 12].

3.2 Transmission electron microscopy (TEM)

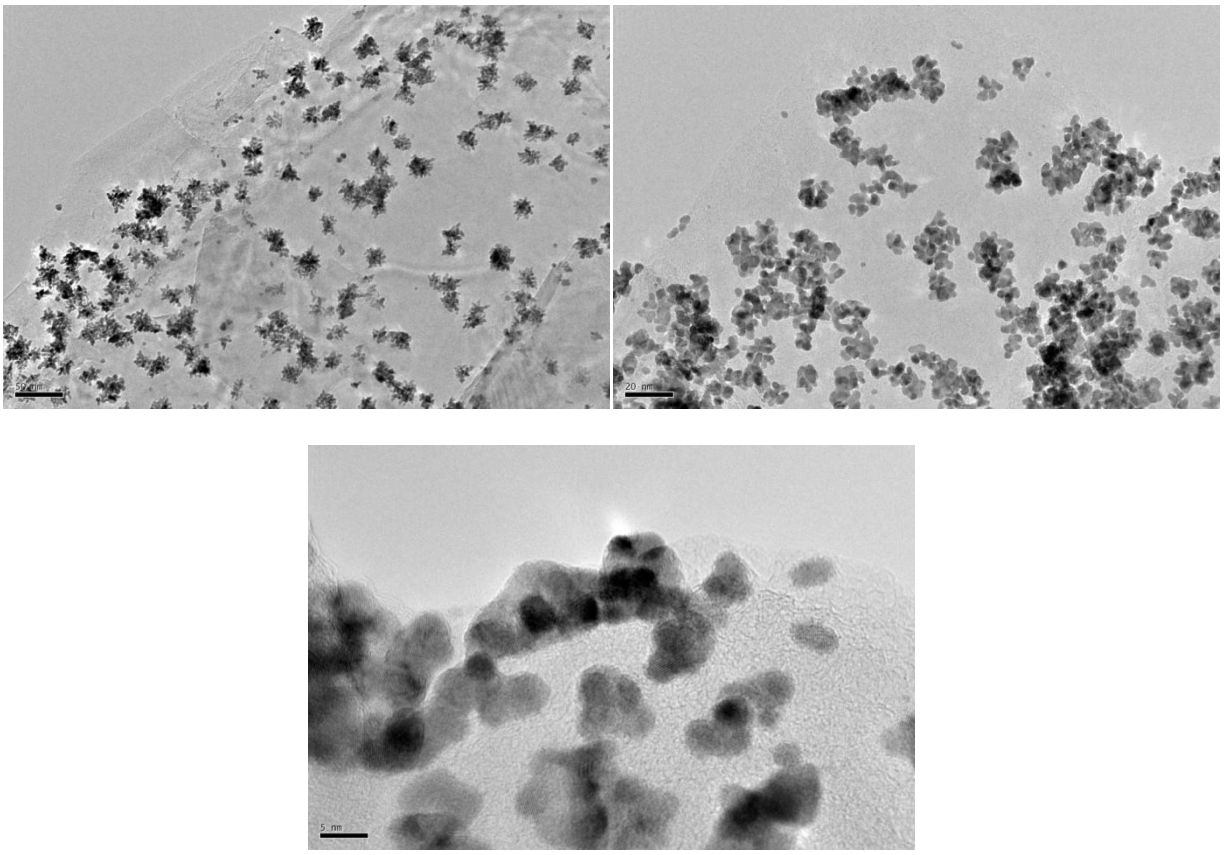

Figure 2. TEM images of the selected $Rh_5@Pt_5/C$ catalyst with different magnifications.

Figure 2 shows the TEM images of sample $Rh_5@Pt_5/C$ with different magnifications. It is clearly seen that a large amount of clusters formed by $Rh_5@Pt_5$ nanoparticles distributed randomly on graphite surfaces, which could be explained by the relatively high surface energy and strong interaction of the nanoparticles. It could be also deduced from the TEM images that Pt was grown on the rough surfaces of Rh nanoparticles previously deposited instead of on the graphite surfaces directly during the second step of hydrogen reduction process, which is well consistent with the result we had obtained [10]. There is no obvious evidence from the TEM images shows that core-shell structure formed according to ref.[21], and the distorted star-like islands of the nanoparticles even indicates that the synthesized catalyst nanoparticles were somewhat less crystallinity and lattice fringe of the face-centered cubic lattice structure, however, our PtRh bimetallic catalyst could be an effective catalyst for the oxidation reaction which will be discussed in the electrocatalytic oxidation of ethanol.

3.3 Cyclic voltammetric characterization

Figure 3 shows the cyclic voltammograms (CV) of Pt_5/C, Rh_5/C and $Rh_5@Pt_x/C$ catalysts with different content of Pt shell in 0.1 M H_2SO_4. The peaks at ca. -0.16 V for all the $Rh_5@Pt_x/C$ samples assigned to hydrogen adsorption/desorption on Rh(110) and Pt(110) planes systematically developed with an increase of Pt content from x = 1 to 5. The electric double layer areas of $Rh_5@Pt_x/C$ catalysts are much broader in comparison to those of Pt_5/C and Rh_5/C, meaning the increased surface roughness of Pt shell which is covered on Rh core.

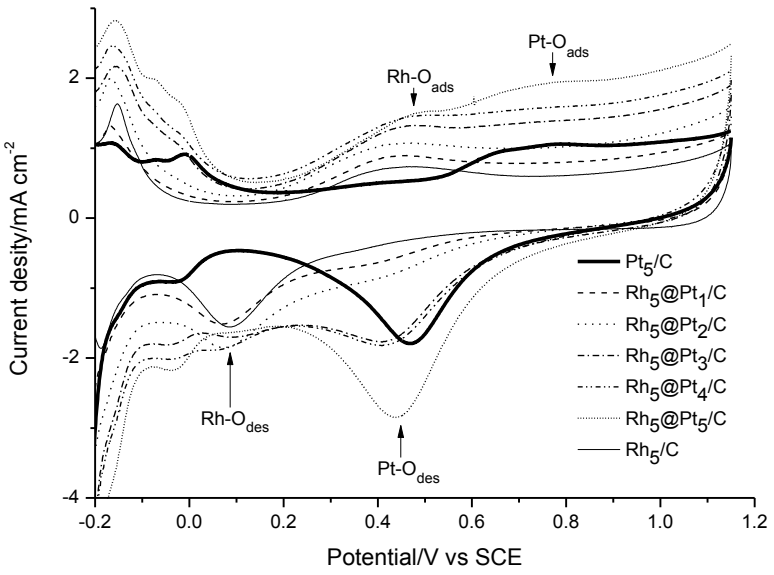

Figure 3. Cyclic voltammograms of Pt_5/C, Rh_5/C and various $Rh_5@Pt_x/C$ catalysts in 0.1 M H_2SO_4 at sweep rate of 10 mVs^{-1}.

Concerning the oxygen reduction peak area during the positive sweep, it is obviously seen that peaks corresponding to $Rh\text{-}O_{ads}$ positively shift from 0.43 to 0.47V and become flatter meanwhile

those corresponding to Pt-O_{ads} strengthen with the increase of Pt content in the shell. Correspondingly, the reduction peaks of Rh-O_{des} at 0.08 V weaken and broaden orderly and shift positively with various Pt increase whereas the reduction peaks of Pt-O_{des} strengthen gradually and positively shift from 0.40 to 0.44 V (still negative to that of 0.50V for Pt_5/C), indicating to a strong interaction between Rh core and Pt shell.

3.4 Electrocatalytic oxidation of ethanol

The anodic potential sweeps for ethanol electrocatalytic oxidation on Pt_5/C, Rh_5/C and $Rh_5@Pt_x$/C with different Pt contents in Pt shell are illustrated in Figure 4. It was already known that there are two main oxidation peaks for ethanol oxidation on the Pt_5/C, shown as the thick solid line, peak A takes place at 0.61 V indicating the oxidation of ethanol to acetaldehyde, acetic acid and CO_2 while peak B at ca. 1.00 V is assigned to the formation of acetic acid, indicating that the end product of ethanol oxidation is mainly acetic acid [24, 26].

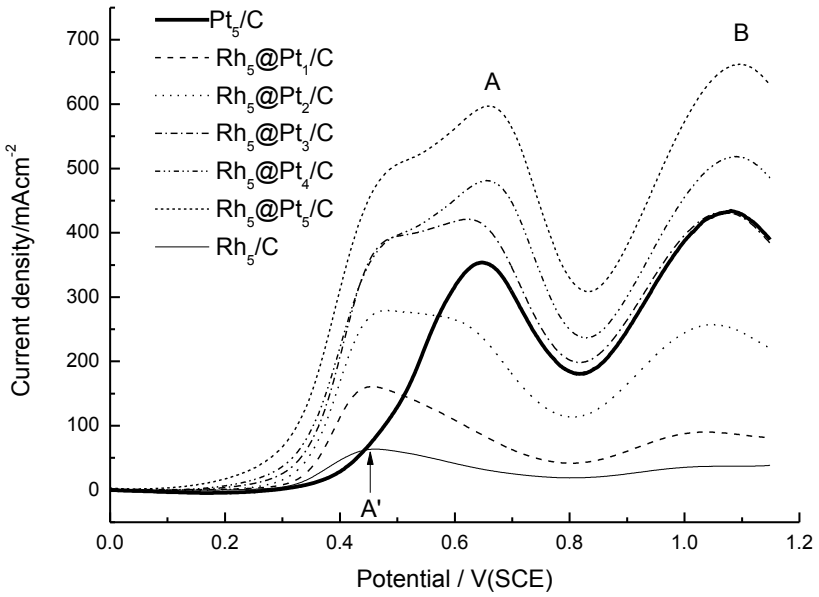

Figure 4. Cyclic voltammograms of ethanol oxidation on Pt_5/C, Rh_5/C and various $Rh_5@Pt_x$/C catalysts in 0.1 M H_2SO_4 + 0.1 M CH_3CH_2OH at sweep rate of 10 mVs^{-1}.

For Rh_5/C, a new peak (marked as peak A') presents at ca. 0.45 V which is 0.20 V negatively shifts from that of peak A for Pt_5/C, which is ascribed to ethanol oxidation occurred on Rh surface. Even though the current density of peak A' is relatively weak, indicating that the main product is CO_2 for ethanol oxidation on pure Rh surface and this further confirms the special C-C bond breaking function of Rh[19-23]. When the Rh core started to be covered by Pt layer such as $Rh_5@Pt_1$/C, both peak A' and A together with peak B appear, which could be ascribed to ethanol oxidation occurred on

both metal surfaces. Furthermore, an increase of peak A' and A with the thickness of Pt shell from x = 1 to 5 positively shifts in order. The peak A is noticeable stronger than peak A' after x = 3 ($Rh_5@Pt_3/C$) and peak A' grows to be a shoulder peak for $Rh_5@Pt_4/C$ and $Rh_5@Pt_5/C$, indicating that Rh core was practically covered by Pt shell. In addition, peak B also develops into stronger with the increase of Pt shell and shows the same oxidation characteristic peaks as those for Pt_5/C indicating the Rh core was entirely covered by Pt. This can be further explained that the partial oxidation of ethanol with production of acetic acid dominantly occurred on Pt surface and it can be concluded that exceedingly thick Pt shell would hinder the enhancement of the Rh to the breaking of C-C bonds. Noticeably, the current density of ethanol oxidation peaks on $Rh_5@Pt_5/C$ is ca. 64 % higher than that on Pt_5/C even though they both show roughly similar characteristic peaks, which indicate the exceptional enhancement of Rh core on the electrocatalytic activity of Pt.

4. CONCLUSION

$Rh_5@Pt_x/C$ core-shell nanoparticles were prepared by a two-step hydrogen reduction process and the effects of the thickness of Pt shell on the catalytic performance for ethanol oxidation were determined. It was found that the Rh cores were gradually covered by various Pt shell thickness, and there was a strong interaction between Rh and Pt. Rh core remarkably enhanced the catalytic activity of Pt shell and promoted the breaking of C-C bonds of ethanol at relatively lower potential. Consequently, the current density of ethanol oxidation peak on $Rh_5@Pt_5/C$ was ca. 64 % higher than that on Pt_5/C although they both showed about similar characteristic peaks.

ACKNOWLEDGEMENTS
We wish to thank the financial support from the Natural Science Foundation of Shanxi Province (No. 2014011003), the Shanxi Scholarship Council of China (No. 2012-006) and Department of Chemistry, Faculty of Science, Chiang Mai University, Thailand.

References

1. S. M. M. Ehteshami and Siew Hwa Chan, *Electrochim. Acta*, 93 (2013) 334.
2. T. C. Blanco, A. R. Pierna and J. Barroso, *J. Power Sources*, 196 (2011) 4337.
3. M. Li, W. P. Zhou, N. S. Marinkovic, K. Sasaki and R. R. Adzic, *Electrochim. Acta*, 104 (2013) 454.
4. E. Higuchi, T. Takase, M. Chiku and H. Inoue, *J. Power Sources*, 263 (2014) 280.
5. Y. W. Lee and K. W. Park, *Catal. Commun*, 55 (2014) 24.
6. W. J. Zhou, Z. H. Zhou, S. Q. Song, P. Tsiakaras and Q. Xin, *Appl. Catal. B: Environ.*, 46 (2004) 273.
7. M. H.M.T. Assumpção, R. M. Piasentin, P. Hammer, R. F.B. De Souza, G. S. Buzzo, M. C. Santos, E. V. Spinacé, A. O. Neto and J. C. M. Silva, *Appl. Catal. B: Environ.*, 174 (2015) 136.
8. D. A. Cantane, W. F. Ambrosio, M. Chatenet and F. H. B. Lima, *J. Electroanal. Chem.*, 681 (2012) 56.
9. Z. L. Liu, X. Y. Ling, X. D. Su, J. Y. Lee and L. M. Gan, *J. Power Sources*, 149 (2005) 1.
10. L. Fang, F. J. Vidal-Iglesias, S. E. Huxter, G. A. Attard and P.B.Wells, *Surf. Sci.*, 631 (2015) 258.

11. R. T. S. Oliveira, M. C. Santos, L. O. S. Bulhões and E. C. Pereira, *J. Electroanal. Chem.*, 569 (2004) 233.
12. L. Fang, F. J. Vidal-Iglesias, S. E. Huxter and G. A. Attard, *J. Electroanal. Chem.*, 622 (2008) 73.
13. F.H.B. Lima, D. Profeti, W.H. Lizcano-Valbuena, E.A. Ticianelli, E.R. Gonzalez, *J. Electroanal. Chem.*, 617 (2) (2008) 121.
14. Kowal, S.L. Gojkovic, K.S. Lee, P. Olszewski, Y.E. Sung, *Electrochem. Commun.* 11(4) (2009) 724.
15. F. H. B. Lima and E. R. Gonzalez, *Electrochim. Acta*, 53 (2008) 2963.
16. S. S. Gupta and J. Datta, *J. Electroanal. Chem.*, 594 (2006) 65.
17. F. H. B. Lima and E. R. Gonzalez, *Appl. Catal. B: Environ.*, 79 (2008) 341.
18. Q. Yuan, Z. Y. Zhou, J. Zhuang and. X. Wang, *Chem. Mater.*, 22 (2010) 2395.
19. H. Wang, C. W. Xu, F. L. Cheng, M. Zhang, S. Y. *Wang and S. P.* Jiang, *Electrochem. Commun.*, 10 (2008) 1575.
20. H. L. Gao, S. J. Liao, J. H. Zeng and Y. C. Xie, *J. Power Sources*, 196 (2011) 54.
21. S. Alayoglu and B. Eichhorn, *J. Am. Chem. Soc.*, 130, (2008) 17479.
22. Y. N. Wu, S. J. Liao, Z. X. Liang, L. J. Yang and R. F. Wang, *J. Power Sources*, 19 (2009) 805.
23. N. Kristian and X. Wang, *Electrochem. Commun.*, 10 (2008) 12.
24. F. J. Vidal-Iglesias, A. Al-Akl, D. J. Watson and G. A. Attard, *Electrochem. Commun.*, 8 (2006) 1147.
25. G. E. Rhead, M. G. Barthès and C. Argile, *Thin Solid Films*, 82 (1981) 201.
26. L. Fang, X. P. Huang, F. J. Vidal-Iglesias, Y. P. Liu and X. L. Wang, *Electrochem. Commun.*, 13 (2011) 1309.